Analogue Sandbox Scaled Modelling of Oblique and Orthogonal Extension Rifting in Rukwa Rift Basin, Tanzania

Tonny Ojok*, John BK Duot, Majorine Namaganda, Nasra Sadiki and Michael Msabi
Department of Geology, College of Earth Sciences & Engineering, University of Dodoma,
P.O. Box 11090 Dodoma, Tanzania
*Corresponding author, E-mail: ojok.tonny1@gmail.com

Abstract

Fault evolution in oblique and orthogonal rift systems in the brittle upper crust of the Rukwa rift basin was simulated using scaled sandbox modelling by varying the angle between the rift axis and the extension direction, α, through 45° and 90°, over a 10 cm displacement. The 45° oblique model exhibits a half-graben architecture bounded by a planar fault, intra-rift faults and a conjugate fault in some vertical sections. The map view of the model's basin trends in the NW-SE direction, and is comparable with the Rukwa rift basin orientation. The 90° oblique model forms a basin structure which is orthogonal to the extension direction of the model in aerial photos. Its linear fault remains orthogonal to the extension direction, while the flexural side of the model segments into sinuous normal faults. Planar to slightly curved intra-rift faults are observed in vertical sections. The half-grabens have similar geometries in vertical sections for both models, while intra-rift faults elongate in vertical sections. The results of the oblique model are similar to natural examples of rift fault systems like the Rukwa rift. The fault geometries of the sandbox models can serve as examples for recognizing fault styles in oblique rift systems.

Keywords: Analogue Sandbox modelling, Oblique rifting, Orthogonal rifting, Tanganyika-Rukwa-Malawi Rift Segment, Rukwa Rift Basin.

Introduction

Experiments with analogue modelling of continental rift structures date back to the 1980s (Withjack and Jamison 1986). Many researchers followed suit (Tron and Brun 1991, McClay and White 1995, McClay et al. 2002, 2005), intending to document and explain basin boundary and internal structure evolution processes. The results from analogue models are then compared to natural phenomena in order to understand geological processes and replicate the action of a given geological scenario (Vidal et al. 2008).

Although the research literature and findings on the Rukwa Rift Basin (RRB) (Morley et al. 1992, Vittori et al. 1997, Morley et al. 2000, Fernandez et al. 2001, Chorowicz 2005, Roberts et al. 2010, 2012, Delvaux et al. 2012, Mtelela 2016) attempt to geologically characterize the basin, they do not pinpoint its true extension direction. Delvaux (2001) notes that the shifts in the basin's extension direction are due to the Rukwa rift basin's multistage evolution since the Late Palaeozoic, while Morley et al. (1992) rule out strike-slip movement due to the lack of folds and reverse faults within the rift and rather suggests oblique movement exhibited by the dominance of extensional features such as full and half-grabens with normal faulting within the Rukwa rift. The RRB, therefore, provides an opportunity to test the applicability of both orthogonal and oblique rift systems, where the former would

exhibit long extensional normal faults while the latter would show a more segmented pattern.

This study used analogue sandbox methods to simulate extension within the Rukwa Rift Basin, with an emphasis on modelling oblique and orthogonal extension within the basin, observing the structures produced in both models, and comparing the model results with the structure of the Rukwa basin. This paper aimed at investigating the dominant extension direction within the Rukwa basin, which was achieved by modelling the aforementioned extension directions within the basin using the scaled analogue sandbox method.

Study Area

The Rukwa Rift Basin (RRB) (Figure 1) is 360 km long and 60 km wide, with up to 12 km of sediment fill (Morley et al. 1999). The basin is located in southwestern Tanzania and is part of the Tanganyika-Rukwa-Malawi (TRM) rift segment of the East African Rift System (EARS). It is occupied in its south-eastern part by a large but shallow lake. The basin is a down-to-northeast half-graben (Kilembe and Rosendhal 1992), bounded by the Lupa fault and Tanzanian craton to the northeast, the Ubende plateau to the north, the Ufipa fault and uplifted Ufipa block to the southwest, and the Mbozi block and Rungwe volcanic province to the south and southeast, respectively. The basin is situated along the trend of the late Ubende basement, which is a well-documented region of crustal structural weakness composed of different terrains arranged in NW–SE lateral shear patterns as reported by Boven et al. (1999). Multiple phases of tectonic reactivation have been established and linked to various tectonic events along the Ubendian belt. The precise timing, course, and structural regime associated with rifting have been ardently debated (Morley et al. 1999). Delvaux et al. (1998) elucidated the debate by pointing out that during the poly-phase rift's existence, various shifts in stress regime and kinematics occurred.
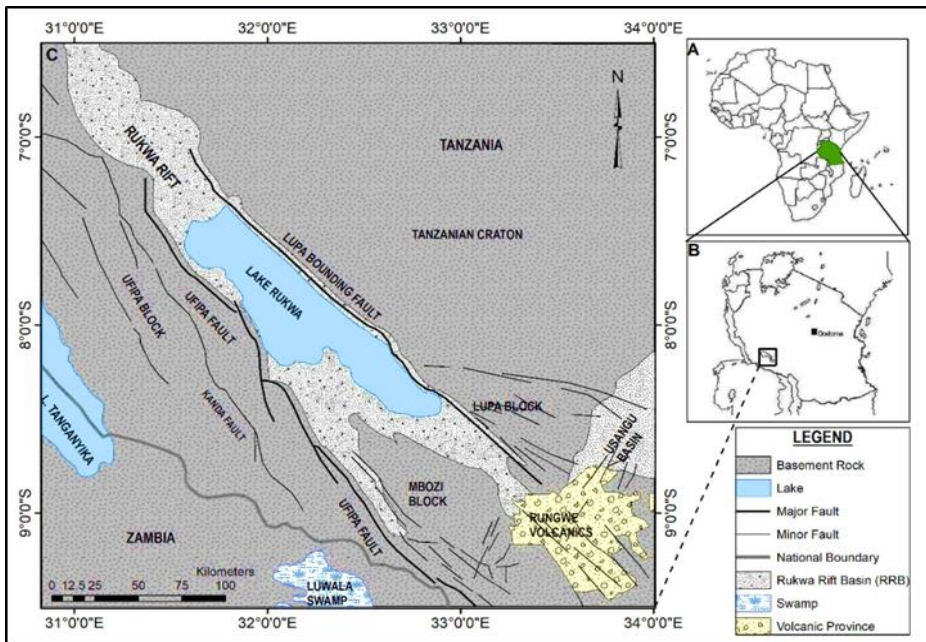
Figure 1: **A**: Location of Tanzania; **B**: Location of the study area (Black square) in Tanzania **C**: RRB showing the linear Lupa and segmented Ufipa border faults (Modified from Delvaux 2001).

Surface geology and stratigraphy of the Rukwa Rift Basin

According to Morley et al. (1992), the Rukwa rift is fully enclosed and fed by drainage from fault-bounded rift flanks made of Precambrian-Pan African crystalline rocks, and its eastern valley forms the main part of the southern Rukwa trough before it is terminated to the southeast by the Tertiary Rungwe volcanics. The basin's seismic profiles revealed up to 12 km of sedimentary fill, making it one of Africa's thickest continental rift-fill basins (Kilembe and Rosendahl 1992).

Seismic profiles, well details, and surface geology all show the accumulation of three tectonically controlled sedimentary sequences within the Rukwa Rift (Kilembe and Rosendahl 1992, Morley et al. 2000, Roberts et al. 2010, Mtelela 2016, Lemna et al. 2019). The lowest unit, which is part of the Karoo Supergroup, reflects continental strata deposition during the Pangaean mega-series. The Lake Beds (Quennell et al. 1956) are the upper sedimentary succession, which records Neogene to Holocene rift-filling associated with the formation of the modern East African Rift System. The middle sedimentary succession, traditionally known as the Red Sandstone Group, is made up of a thick package of continental sandstones and subordinate mudstones of disputed age. A brief description of the sedimentary sequences (Figure 2) is presented below.

Karoo Supergroup

In southeast Tanzania, the Rukwa Rift's Karoo exposures are sparse, ranging from the Songwe-Kiwira region near the Malawi border in the south to isolated outcrops near Songwe, Galula, Muze, Namwele, and Usevia areas (O'Connor et al. 2019). The Karoo sediments are in fault contact with the crystalline basement in these regions (Morley et al. 1992). According to Semkiwa et al. (1998), the Karoo Supergroup in the Rukwa Rift is made up of about 3 km of a collection of glacial, lacustrine, and fluvial deposits that range in age from late Carboniferous to late Permian (Figure 2). Thin diamictites, heavy oxidized mudstones and sandstones, and

extensive coal deposits dominate this group (Dypvik et al. 1990).
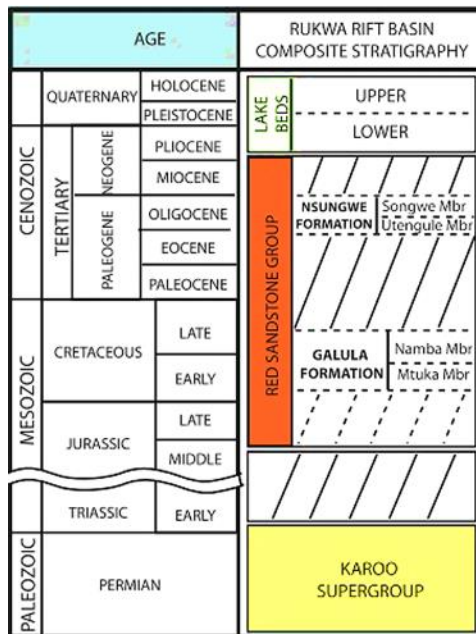
Figure 2: Composite stratigraphy within the RRB (Adopted from Roberts et al. 2010).

Red Sandstone Group (RSG) depositional sequence

The RSG, which is primarily composed of fluvial and alluvial fan deposits (Morley et al. 1992), overlies the Karroo, with an angular unconformity (Figure 2) averaging 15° on the rift margins. The group comprises a Cretaceous fluvial lower part referred to as the Galula Formation and a fluvio-lacustrine upper part called the Nsungwe Formation (Figure 2) (Roberts et al. 2010, 2012). The RSG thickness varies across the basin, with outcrop exposures varying from 600 m to 3 km on the basin's western margin (Kilembe and Rosendahl 1992, Roberts et al. 2010). The age of the Red Sandstone Group, though traditionally controversial, has been refined by more recent papers like Roberts et al. (2010, 2012). They refined our understanding of the Red Sandstone Group as comprising, in part, the Mid Cretaceous Galula Formation and the Oligocene Nsungwe Formation. Both have been dated biostratigraphically and in part using detrital Zircon geochronology plus

the radiometrically dated volcanic tuff (Roberts et al. 2010, 2012).

Lake Beds depositional sequence

Morley et al. (1992) note that the Lake Bed Formation is made up of unconsolidated upper Neogene-Quaternary sediments that lie on top of the Red beds. These sediments are characterized by unconsolidated alluvium, sand, silt, and mud, and intercalated volcanic ash. According to Ebinger et al. (1989), the Rukwa Rift Basin's Lake Beds succession was deposited in response to modern tectonism of the East African Rift System (EARS) and it is the basin's youngest mega-sequence. Lake Beds strata in the Rukwa Basin are mostly exposed in the Galula region. The Lake Beds thicken significantly towards the east, reaching a maximum thickness of 4 kilometres along the Lupa bounding fault (Roberts et al. 2010).

Structural Style and Tectonic Evolution

The Rukwa basin's stratigraphy and composition are relatively well understood (Wescott et al. 1991, Kilembe and Rosendahl 1992, Morley et al. 1992). The Precambrian basement of the Rukwa is 4,000 m deep in its northern half, and 11,000 m deep in its southern half (Peirce and Lipkov 1988, Morley et al. 1992). The northern portion of the Rukwa basin appears as a symmetric graben (Rosendahl et al. 1992) and the basin divides into two opposing half-grabens separated by the Mbozi block as it moves southwards, with sedimentary layers diverging towards the boundary faults. The evolution of the Rukwa rift is linked to the formation of the NW-SE trending Palaeoproterozoic Ubende fabric along the western margin of the Archean Tanzanian craton (Lenoir et al. 1994, Theunissen et al. 1996).

The Rukwa Basin's tectonic evolution is associated with several rifting episodes in late Carboniferous-Permian (Karoo), Cretaceous (Lower RSG), Paleogene (upper RSG), and Neogene (Lake Beds) times (Roberts et al. 2010, 2012, Delvaux et al. 2012, Lemna et al. 2019). Karoo rifts cut through the EARS from the Late Carboniferous to the Early Triassic

periods. Karoo basins contain Late Carboniferous to Late Permian sediments, but they lack Triassic sediments (Dypvik et al. 1990). Karoo sedimentation was most likely controlled by the Ubende fabric's transpressional reactivation (Mbede 1993, Theunissen et al. 1996, Klerkx et al. 1998). Delvaux et al. (1998) note that deposition of Karoo sediments along the Rukwa accommodation zone ended during the Late Permian. A second rifting event in the Rukwa occurred during the Late Jurassic and Cretaceous and is linked with the deposition of the lower fluvial Red Sandstone Group sequence (Roberts et al. 2010, 2012). A third rifting event occurred in the late Oligocene, resulting in the deposition of the fossiliferous fluvio-lacustrine upper Red Sandstone Group sequence (Roberts et al. 2010, 2012). The Red Sandstone Group is thought to have formed during a period of pure extensional faulting, with a horizontal principal extension oriented NE-SW and orthogonal to the Tanganyika-Rukwa-Malawi (TRM) rift axis (Delvaux et al. 1992, Damblon et al. 1998). Up to 10 km of extension of the Tertiary segment in a direction oblique to the likely E-W regional extension direction is indicated by NE-SW seismic lines (Morley et al. 1992). The Late Cenozoic rifting cycle is divided into two first-order phases separated by a tectonic pause in the early Pleistocene. The older Lake Beds are described as late Miocene-Pliocene deposits (Harkin 1955). The predominance of normal faulting under a semi-radial extensional stress regime characterizes this time and it resulted in the reactivation and rapid subsidence of the NW-SE trending south Rukwa Basin (Delvaux et al. 1992).

Materials and Methods
Experimental setup

The experimental models were performed under standard laboratory temperature and pressure conditions of normal room temperature, pressure and controlled light. The setups were carried out in a glass-sided deformed rig of 140 cm long by 50 cm wide and 35 cm deep in which an 11 cm thick-layered sandpack of well-sorted dry white and coloured silica sand on top of: (**a**) a basal

detachment with a 10 cm wide rubber sheet fixed between two fibreboard end sheets and oriented at an angle of 45° to the extension direction and (**b**) a basal detachment formed by a wooden footwall block with a 60° slanting ramp oriented orthogonally to the extension direction (Figure 4). These were used to simulate oblique and orthogonal rift systems in the Rukwa Basin. The models were covered with an absorbent piece of cloth and impregnated with water before marking the model surfaces at 1 cm intervals and cutting the models into serial vertical sections along the markings. Cameras mounted aerially and laterally were used to photograph the models during each of the experiments. The aerial camera was computer-controlled, while the lateral cameras were manually controlled by pre-set camera timers. Camera lights mounted aerially to the deformation rig were used to enhance illumination and aid in the visualization of formed structures on the models' surfaces and sides during extension and in vertical sections.

Methodology

The experimental method followed that described by McClay and Ellis (1987) and applied in other works by McClay and White (1995), McClay et al. (2002), Amilibia et al. (2005). The models were scaled such that they simulate brittle deformation of a sedimentary sequence between 1 and 10 km in thickness (Figure 3) Amilibia et al. (2005). The experiment was carried out in a glass-sided deformation rig (Figure 5) located in the GeoModels laboratory at the College of Earth Sciences and Engineering, University of Dodoma (UDOM), Tanzania.

Four experiments were carried out to study both oblique and orthogonal extension. The basement geometry for the oblique model consisted of a 10 cm rubber anchored between two fibreboard end sheets at an angle (α) of 45° (Figure 4(a)) to the rifting zone, while the orthogonal model consisted of a baseplate formed by a wooden footwall block consisting of a ramp slanting at 60° from the block's edge (Figure 4(b)). These angles were chosen based on the finds of Mahwa (2017), who noted that faults within the Rukwa are of high angles greater than 45°. The models also consisted of an 11 cm thick-layered sandpack formed by alternating sieved white and coloured dry silica sand. The sandpack represented the three sedimentary sequences within the Rukwa basin where the blue-white sand layer represented the Karoo deposition sequence, while the red-white and green-white sand layers represented the Red Sandstone and Lake Bed deposition sequences, respectively (Figures 5 and 6). The models were deformed by moving one motor-driven end wall at a pre-set discontinuous displacement rate of 0.5 cm/min (Figures 5 and 6). After each 0.5 cm of extension, the accommodation space was infilled with alternating layers of white, red and green sand to simulate syn-sedimentation. The models were extended to a maximum of 10 cm in 0.5 cm increments parallel to the long axis of the deformation rig. The model deformation was recorded at constant time intervals by side and overhead mounted 35 mm photography to observe lateral changes of the model through the glass walls of the deformation rig and surface changes as well. Despite the frictional drag along the glass side-walls of the deformation rig, which results in slightly curved surface fault traces at the edges of the model (McClay 1990), the faulting observed through the glass side-walls gives an indication of the style of faulting within the interior of the model. The experiments were repeated for each baseplate configuration to ensure the reliability of the results. It should be noted that this method does not consider the effects of compaction and pore fluid as well as the thermal and flexural effects generated or associated with faulting in the upper crust in nature, and hence these were ignored during modelling.
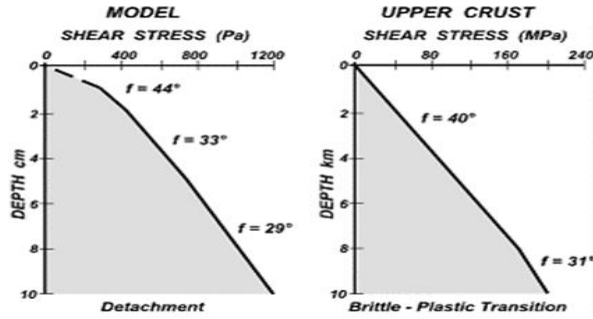
Figure 3: Scaling parameters for the simulation of brittle deformation between model and sedimentary rocks in the upper crust (Adopted from Amilibia et al. 2005).
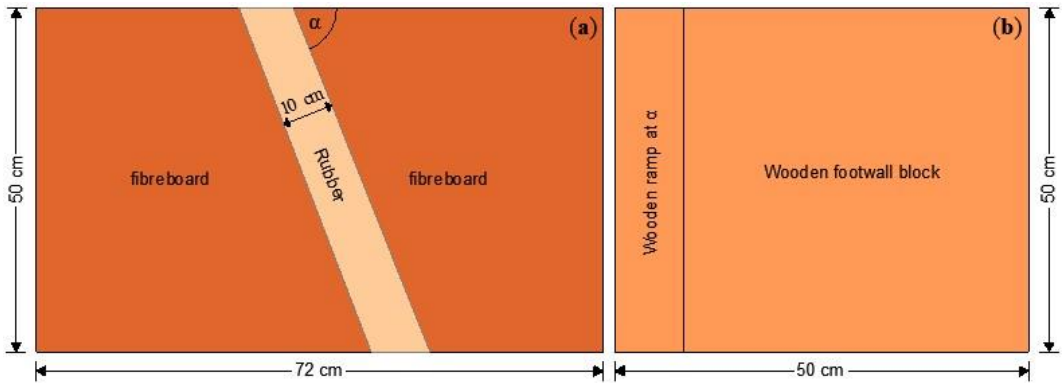
Figure 4: Plan view of basement geometries used for (a) oblique and (b) orthogonal rift modelling.
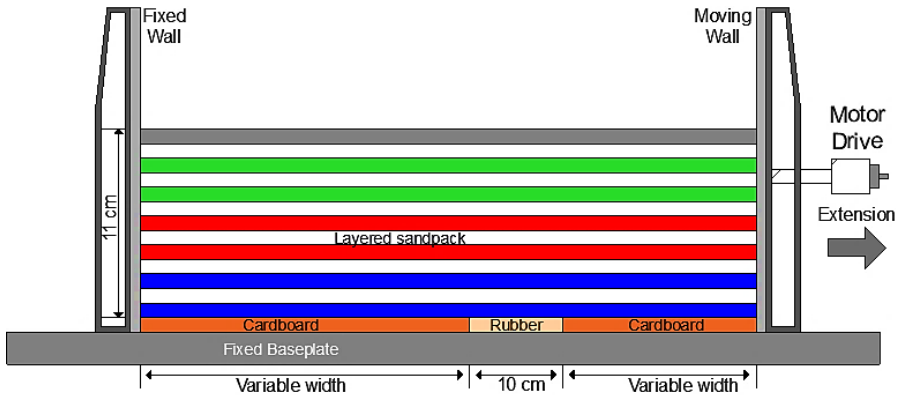
Figure 5: Sketch of basal detachment experiment with rubber oriented at an angle (α) to the extension direction. The blue, red, and green layers represent the three depositional sequences within the Rukwa Basin.
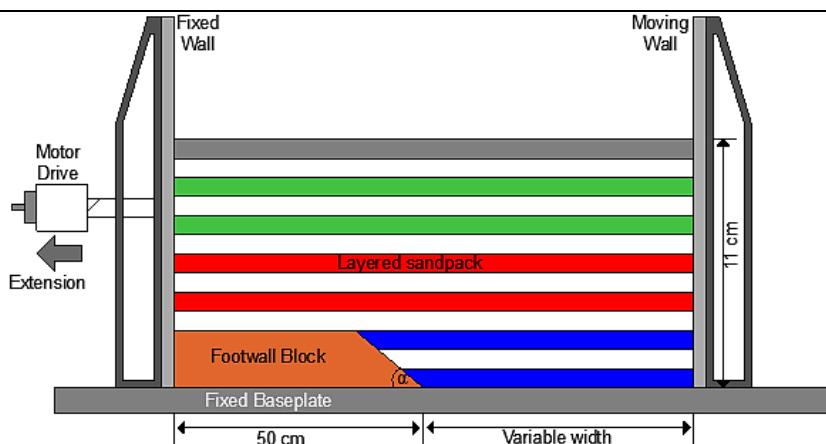
Figure 6: Sketch of the wooden footwall block basal detachment experiment with a ramp inclined at an angle, α. The blue, red, and green layers represent the three depositional sequences within the Rukwa Basin.

Results

For each model, map view photographs, the positions of vertical section photographs taken at 1 cm intervals and their interpretations are presented. The results presented in this paper also have strong similarities with previous works such as McClay and White (1995) and Amilibia et al. (2005).

Oblique rift 45° model

The underlying zone of basement stretching was angled 45° to the direction of extension. The model emerged early in the first 0.5 cm extension, forming two parallel-to-the-rift-axis rift border faults and a normal graben (Figure 7). The left border fault began to form short curvilinear segmented faults, relay ramps, and obscure accommodation zones as the extension increased from 4 cm to 5 cm (Figures 8 and 9). With an increased extension, the fault segments on the flexural side of the model began to coalesce, forming long, curvilinear segments with minor intra-rift faults and relay ramps (Figures 9 and 10). The model was characterized in vertical sections by a half-graben bound by a planar master fault and curvilinear intra-rift faults with domino type faulting and a southeast dip, as well as a conjugate fault set dipping 20° to the left (Figure 11). Also in vertical sections, no rotation of intra-rift faults was observed. During the 10 cm extension, five intra-rift faults were observed to form, with a new fault forming every 2 cm. The first two intra-rift faults are restricted to the blue-white (Karoo) and first layers of the red-white (Red Sandstones) sand packs, which represent Permo-Triassic and Cretaceous rifting events, whereas the later three intra-rift faults extend across the entire red-white (Red Sandstones) and green-white (Lake Beds) successions modelled in the experiment (Figure 11). Sections 4 and 9 of Figure 11 traverse an intersecting conjugate set where a later fault deforms the earlier left dipping fault. Section 20 cuts through two intra-rift faults that intersect to form a potential trap in the green-white sedimentary sequence representing the Rukwa basin's tertiary lake beds (Figure 11). The model's structural style is similar to that seen in seismic line TVZ-14X (Figure 12) and fault patterns seen in other orthogonal rift experiments such as that of McClay and White (1995).
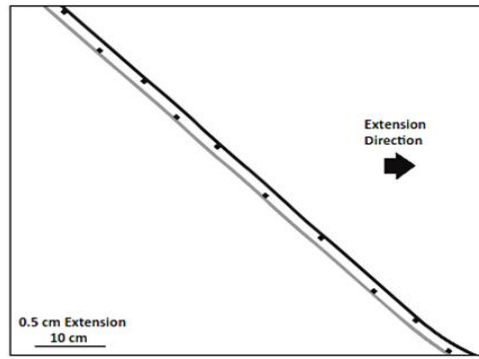
Figure 7: Map view line diagram of the 45° model at 0.5 cm extension. The dark band is the left-dipping rift border fault, while the light band is the right-dipping border normal fault.
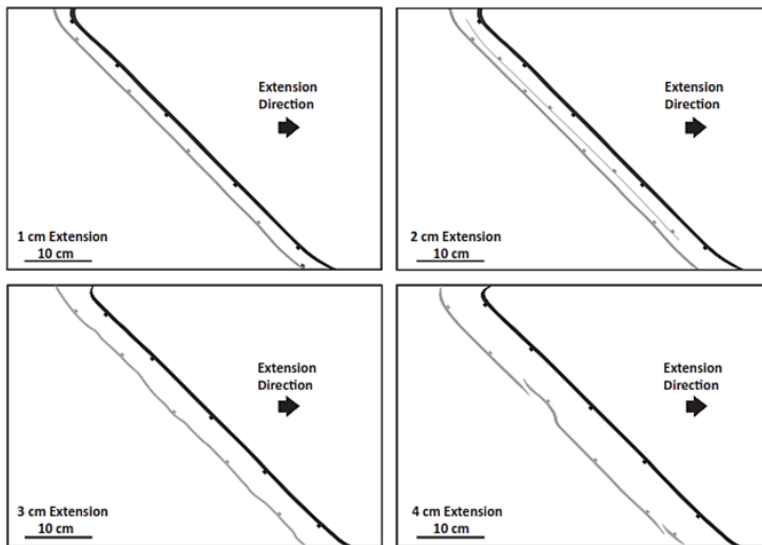
Figure 8: Sequential line diagrams of progressive deformation and fault style on the surface of the 45° oblique rift model after 1, 2, 3, and 4 cm of extension. The dark band is the left-dipping rift border fault, while the light bands are right-dipping border faults and fault segments.
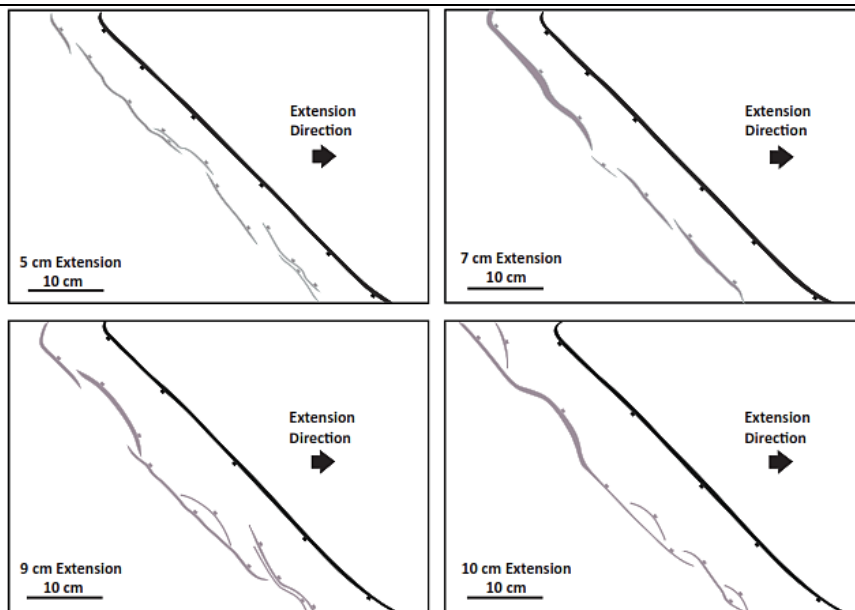
Figure 9: Sequential line diagrams of progressive deformation and fault style on the surface of the 45° oblique rift model after 5, 7, 9, and 10 cm of extension. The dark band is the left-dipping rift border fault, while the light bands are right-dipping segmented border and intra-rift normal faults.
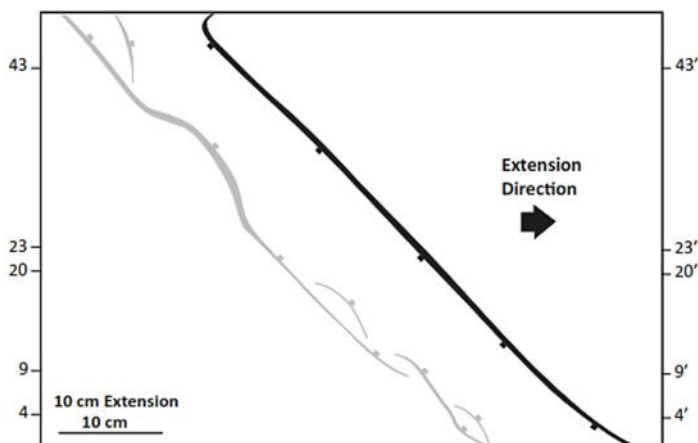
Figure 10: Line diagram of the surface of the 45° model at the end of the extension, indicating the positions of serial vertical sections in Figure 11. The dark band is the left-dipping rift border fault, while the light bands are right-dipping segments of the border normal fault.

Figure 11: Serial vertical sections taken 1 cm apart, orientated parallel to the extension direction through the 45° oblique model.
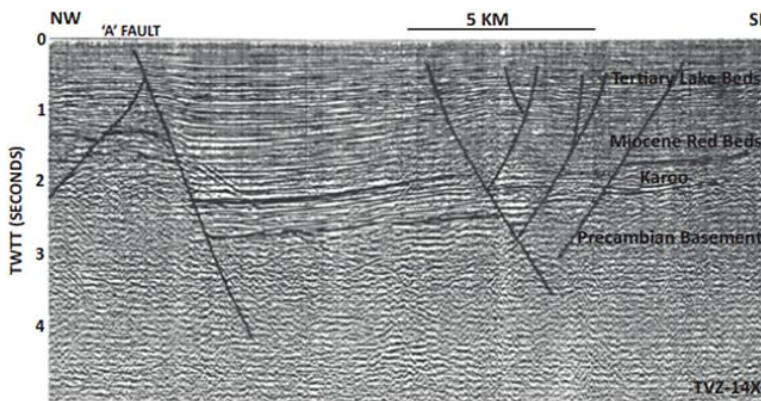
Figure 12: Seismic line TVZ-14X, showing close similarity in the fault pattern to the 45° oblique model experiment (Modified from Morley et al. 1992).

Orthogonal rift 90° model

The underlying zone of basement stretching was oriented 90° to the extension direction. The first 1 cm extension resulted in no visible subsidence or surface faults above the stretching zone. The structural evolution of the rift system began after 1.5 cm of extension, with visible surface faulting and subsidence in the model surface (Figure 13). Long linear rift border faults developed on both margins of the extended zone and perpendicular to the extension direction, spanning the entire width of the model (Figure 13). With increased extension up to 6.5 cm (Figure 14), the left-hand border fault system became more pronounced, while the right-hand rift border fault system began to segment into individual curvilinear normal

faults, forming an overlapping fault system separated by narrow accommodation zones on the right side of the model. These normal faults continued to run perpendicular to the direction of extension and became elongated by along-strike propagation after 6.5 cm extension, forming sinuous fault scarps and relay ramp systems along the model's flexural margin where the faults overlapped each other (Figure 14). Deformation of the model was characterized in serial vertical sections (positions shown in Figure 15) by a half-graben bounded by a planar border fault dipping at 60°, minor subvertical conjugate faults, and intra-rift normal faults dipping at low angles (20°–30°) to the right of the model at the end of a 10 cm extension (Figure 16). Normal faults were initially restricted to the

blue-white and first layers of red-white sand packs, but later faults extended across all three sand packs. Section 19 cuts through a point in the green-white sand pack where two intra-rift faults meet to form a joint (Figure 16).
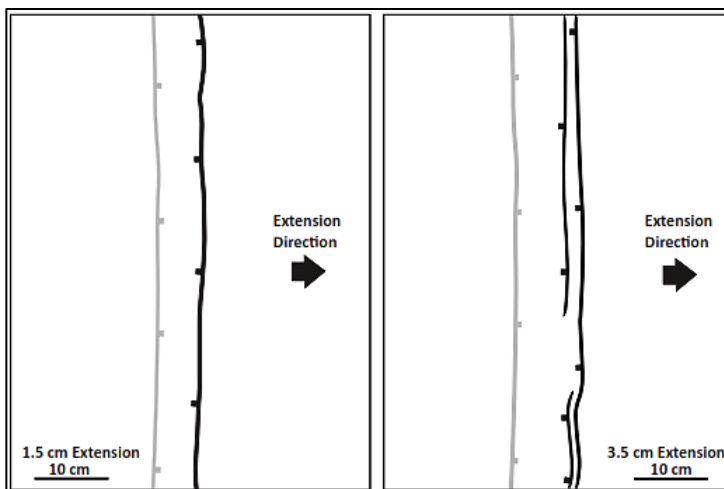
Figure 13: Sequential line diagrams of progressive deformation and fault style on the surface of the 90° orthogonal rift model after 1.5 and 3.5 cm of extension. The dark bands are the left-dipping rift border and intra-rift faults, while the light band is the right-dipping border normal fault.
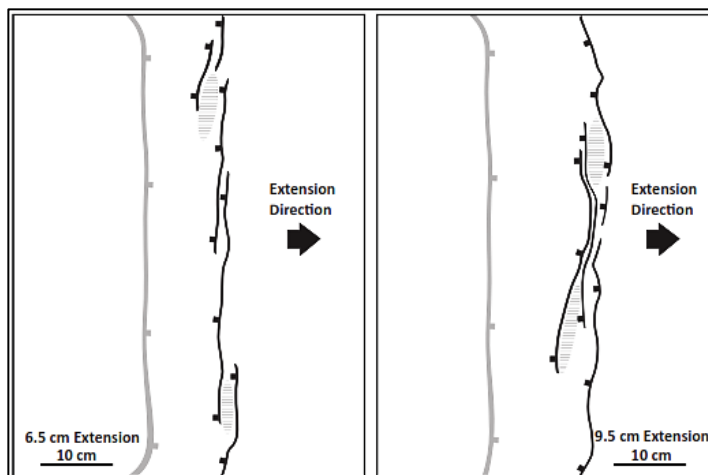
Figure 14: Sequential line diagrams of progressive deformation and fault style on the surface of the 90° orthogonal rift model after 6.5 and 9.5 cm of extension. The dark bands are the left-dipping rift, segmented border, and intra-rift faults, while the light band is the right-dipping border normal fault. Gray hatch lines represent accommodation zones.
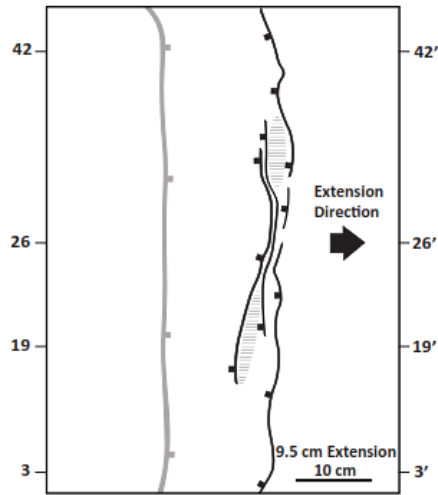
Figure 15: Line diagram interpretation of fault arrays at 9.5 cm extension the 90° model indicating positions of vertical sections in Figure 16. The linear band is a border fault dipping to the left, while the curved bands are intra-rift faults dipping to the right.
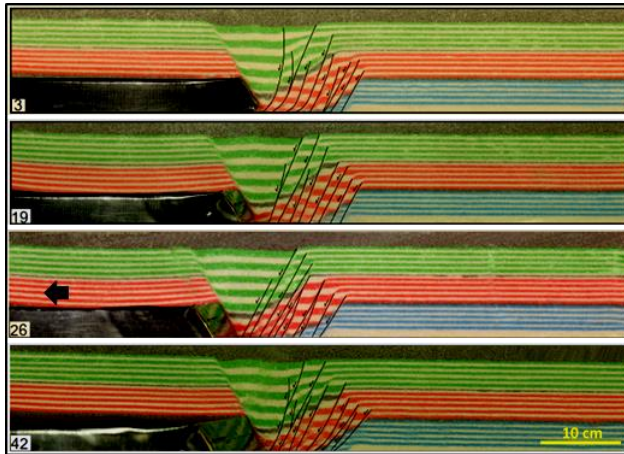
Figure 16: Serial vertical sections taken 1 cm apart parallel to the extension direction through the ($\alpha = 90°$) orthogonal model.

Discussion

The orthogonal rift model was characterized by a long curvilinear rift border fault, an elongated along strike and segmented sinuous border fault, intra-rift faults, and obscure narrow accommodation zones, all of which formed perpendicular to the extension direction. The oblique rift model, on the other hand, was distinguished by a long linear border fault, an along-strike segmented sinuous border fault, and short intra-rift faults that formed parallel to the rift axis and underlying zone of deformation and

differential thinning. The main half-graben in both models had the same geometry in serial vertical sections with the depocenter restricted towards the master boundary fault, while surface faults on the flexural side of both models were elongated by along-strike fault propagation. Moreover, the half-graben style of the Rukwa Basin was also noted by Kilembe and Rosendhal (1992), Morley et al. (1992), Delvaux (2001) and Lemma et al. (2019). The master border fault that formed on the moving wall edge extended across the entire width of the model, whereas the faults

on the flexural margin were segmented with minor relay ramps formed between the segments. The intra-rift faults in the orthogonal model were curvilinear and perpendicular to the extension direction, while in the oblique model, they were mostly concave towards the direction of extension and subparallel to the rift axis. The initial faults in both models extend from the blue-white (Karoo) up to the lower red-white (Red Sandstone) layers (Galula formation) and represent Permo-Triassic and Cretaceous rifting events (Kilembe and Rosendahl 1992, Roberts et al. 2004, 2010), while the subsequent faults extend from the red-white layers (Red Sandstone) and extend across the entire green-white layers (Lake Beds) and represent the Paleogene and Neogene-Recent rifting events as reported by Roberts et al. (2010, 2004) and shown by Figure 11. However, this deduction does not consider the unconformities (Figure 2) which presented a limitation to the modelling. The fault patterns of the oblique model (Figure 11) compare well with the structural style seen in seismic line TVZ-14X (Morley et al. 1992) and the natural Rukwa rift. Figures 11 and 16 portray the linear Lupa boundary and Ufipa segmented boundary fault existing on the Northeast and Southwest margins of the Rukwa Basin, respectively. However, the structural architecture in these models differs from that observed in full graben oblique systems experiments (Keep and McClay 1997, McClay et al. 2002, Corti 2012) which are characterized by sub-basins within symmetric grabens, multiple accommodation zones with interlocking conjugate faults oblique to the extension direction, complex fault arrays, and well-developed relay ramps in places. In both models, the number of extensional faults increased with increased extension angle between the rift zone and extension direction. The surface pattern of the models was controlled by the geometrical angle of the baseplate, which also had a direct impact on the fault arrangement formed

within the models, with more extensional faults forming at higher angles.

Conclusion

In analogue models of half-graben oblique rifts, the first formed extensional fault controls the orientation and distribution of other faults developed during the extension. Additionally, the number of extensional faults formed depends on the oblique angle of deformation and with continued extension, more faults are formed during model deformation. Due to syn-tectonic sedimentation, the principal deformation structure in the 45° oblique model formed as a half-graben bounded by a planar master fault dipping at the same angle to the left and five extensional faults dipping at lower angles to the right, while in the 90° orthogonal model, eight extensional faults dipping at 60° to the left and a planar master fault dipping at the same angle to the right were formed. The master fault formed in the oblique model represents the long linear Lupa fault in nature, while the segmented margin represents the Ufipa fault in nature. The joints formed in the green-white syn-depositional sequence in both models indicate the existing potential traps in the lake beds, as suggested by Mahwa (2017). A detailed study is recommended to compare theoretical diagrams from sandbox models and seismic interpretation to study constraints on displacement profiles and uplift rates with time.

References

Amilibia A, McClay KR, Sabat F, Muñoz JA, and Roca E 2005 Analogue modelling of inverted oblique rift systems. *Geol. Acta* 3(3): 251-271.

Boven A, Theunissen K, Sklyarov E, Klerkx J, Melnikov A, Mruma A, and Punzalan L

1999 Timing of exhumation of a high-pressure mafic granulite terrane of the Paleoproterozoic Ubende belt (West Tanzania). *Precambrian Res*. 93(1): 119-137.

Chorowicz J 2005 The East African rift system. *J. Afr. Earth Sci.* 43(1-3): 379-410.

Corti G 2012 Evolution and characteristics of continental rifting: Analog modeling-inspired view and comparison with examples from the East African Rift System. *Tectonophysics* 522-523: 1-33.

Damblon F, Gerrienne P, D'Outrelepont H, Delvaux D, Beeckman H, and Back S 1998 Identification of a fossil wood specimen in the Red Sandstone Group of southwestern Tanzania: stratigraphical and tectonic implications. *J. Afr. Earth Sci.* 26: 387-396.

Delvaux D 2001 Tectonic and palaeostress evolution of the Tanganyika-Rukwa-Malawi rift segment, East African rift System. *Peri-Tethys Memoir*. 6: 545-567.

Delvaux D, Kervyn F, Macheyeki AS, and Temu EB 2012 Geodynamic significance of the TRM segment in the East African Rift (W-Tanzania): Active tectonics and paleostress in the Ufipa plateau and Rukwa basin. *J. Structural Geol.* 37: 161-180.

Delvaux D, Kervyn F, Vittori E, Kajara RSA., and Kilembe E 1998 Late Quaternary tectonic activity and lake level change in the Rukwa Rift Basin. *J. Afr. Earth Sci.* 26(3): 397-421.

Delvaux D, Levi K, Kajara R, and Sarota J 1992 Cenozoic paleostress and kinematic evolution of the Rukwa-North Malawi rift valley (East African rift system). *Bull. Cent. Rech. Explor.-Prod. Elf-Aquitaine* 16(2): 383-406.

Dypvik H, Nesteby H, Ruden F, Aagaard P, Johansson T, Msindai J and Massay C 1990 Upper paleozoic and Pesozoic sedimentation in the Rukwa-Tukuyu Region, Tanzania. *J. Afr. Earth Sci.* 11(3-4): 437-456.

Ebinger CJ, Deino AL, Drake RE and Tesha AL 1989 Chronology of volcanism and rift basin propagation: Rungwe volcanic province, East Africa. *J. Geophys. Res.: Solid Earth*. 94(B11): 15785-15803.

Fernandez-Alonso M, Delvaux D, Klerkx J and Theunissen K 2001 Structural link between Tanganyika-and Rukwa-rift basins at Karema-Nkamba (Tanzania): basement structural control and recent evolution. *Mus.* *Roy. Afr. Centr., Tervuren (Belgique), Dép. Géol. Min., Rap. Ann*. 91-100.

Harkin DA 1955 The geology of the Songwe-Kiwira coal field, Rungwe District. *Geol. Surv. Tanganyika Bull.* 27: 17.

Keep M and McClay KR 1997 Analogue modelling of multiphase rift systems. *Tectonophysics* 273: 239-270.

Kilembe EA and Rosendahl BR 1992 Structure and stratigraphy of the Rukwa rift. *Tectonophysics* 209(1-4): 143-158.

Klerkx J, Theunissen K and Delvaux D 1998 Persistent fault controlled basin formation since the Proterozoic along the Western Branch of the East African Rift. *J. Afr. Earth Sci.* 26(3): 347-361.

Lenoir JL, Liégeois JP, Theunissen K and Klerkx J 1994 The Palaeoproterozoic Ubendian shear belt in Tanzania: Geochronology and structure. *J. Afr. Earth Sci.* 19(3): 169-184.

Lemna OS, Stephenson R and Cornwell DG 2019 The role of pre-existing Precambrian structures in the development of Rukwa Rift Basin, southwest Tanzania. *J. Afr. Earth Sci.* . 150: 607-625.

Mahwa J 2017 *Structural framework and its effects on traps formation in the south-eastern part of Rukwa basin*. MSc Dissertation, University of Dodoma, Tanzania.

Mbede EI 1993 *Tectonic development of the Rukwa Rift basin in SW Tanzania*. PhD thesis, Technische Universität Berlin.

McClay KR 1990 Extensional fault systems in sedimentary basins: a review of analogue model studies. *Marine Petrol. Geol.* 7(3): 206-233.

McClay KR and Ellis PG 1987 Geometries of extensional fault systems developed in model experiments. *Geol.* 15(4): 341-344.

McClay KR and White MJ 1995 Analogue modelling of orthogonal and oblique rifting. *Marine Petrol. Geol*. 12(2): 137-151.

McClay KR, Dooley T, Whitehouse P and Mills M 2002 4-D evolution of rift systems: Insights from scaled physical models. *AAPG Bull*. 86(6): 935-959.

McClay KR, Dooley T, Whitehouse PS and Anadon-Ruiz S 2005 4D analogue models of extensional fault systems in asymmetric rifts: 3D visualizations and comparisons with natural examples. In: Geological Society of London *Petrol. Geol. Conf. Ser.*

6(1): 1543-1556.

Morley CK, Cunningham SM, Harper RM and Wescott WA 1992 Geology and geophysics of the Rukwa rift, East Africa. *Tectonics* 11(1): 69-81.

Morley CK, Ngenoh DK, Ego JK 1999 *Introduction to the East African Rift System*. In: Morley CK (Ed) Geoscience of Rift Systems-Evolution of East Africa. *AAPG Studies in Geol*. 44: 1-18.

Morley CK, Vanhauwaert P and De Batist M 2000 Evidence for high-frequency cyclic fault activity from high-resolution seismic reflection survey, Rukwa Rift, Tanzania. *J. Geol. Soc.* 157(5): 983-994.

Mtelela C 2016 *Sedimentology and stratigraphy of the late Cenozoic lake beds succession, Rukwa Rift Basin, Tanzania: implications for hydrocarbon prospectivity*. PhD Dissertation, James Cook University.

O'Connor PM, Krause DW, Stevens NJ, Groenke JR Macphee RD, Kalthoff DC and Roberts, EM 2019 A new mammal from the Turonian–Campanian (Upper Cretaceous) Galula Formation, southwestern Tanzania. *Acta Palaeontologica Polonica* 64(1).

Peirce JW and Lipkov L 1988 Structural interpretation of the Rukwa rift, Tanzania. *Geophysics* 53(6): 824-836.

Quennell AM 1956 The Bukoban System of East Africa. In: Cong XX. *Geol. Intern*. *El Sistema Cambrico, Symp.* 1(1): 281-307.

Roberts EM, Stevens NJ, O'Connor PM., Dirks PHGM, Gottfried MD, Clyde WC and Hemming S 2012 Initiation of the western branch of the East African Rift coeval with the eastern branch. *Nat. Geosci*. 5: 289-294.

Roberts EM, O'Connor PM, Stevens NJ, Gottfried MD, Jinnah ZA, Ngasala S and Armstrong RA 2010 Sedimentology and depositional environments of the Red Sandstone Group, Rukwa Rift Basin, southwestern Tanzania: New insight into Cretaceous and Paleogene terrestrial ecosystems and tectonics in sub-equatorial Africa. *J. Afr. Earth Sci.* 57(3): 179-212.

Roberts EM, O'Connor PM, Gottfried MD, Stevens N, Kapalima S, and Ngasala S 2004 Revised stratigraphy and age of the Red Sandstone Group in the Rukwa Rift Basin, Tanzania. *Cretaceous Res*. 25(5): 749–759.

Rosendahl BR, Kilembe E and Kaczmarick K 1992 Comparison of the Tanganyika, Malawi, Rukwa and Turkana rift zones from analyses of seismic reflection data. *Tectonophysics* 213(1-2): 235-256.

Semkiwa P, Kalkreuth W, Utting J, Mayagilo F, Mpanju F and Hagemann H 1998 The geology, petrology, palynology and geochemistry of Permian coal basins in Tanzania. 1. Namwele-Mkomolo, Muze and Galula coalfields. *Int. J. Coal Geol.* 36: 63-110.

Theunissen K, Klerkx J, Melnikov A and Mruma A 1996 Mechanisms of inheritance of rift faulting in the western branch of the East African Rift, Tanzania. *Tectonics* 15(4): 776-790.

Tron V and Brun JP 1991 Experiments on oblique rifting in brittle-ductile systems. *Tectonophysics* 188(1-2): 71-84.

Vidal-Royo O, Ferrer O, Koyi H, Vendeville BC, Muños JA and Roca E 2008 3D reconstruction of analogue modelling experiments from 2D datasets. *Boll. Geofis. Teor. Appl.* 49(2): 524-528.

Vittori E, Delvaux D and Kervyn F 1997 Kanda fault: A major seismogenic element west of the Rukwa Rift (Tanzania, East Africa). *J. Geodynamics* 24(1-4): 139-153.

Wescott WA, Krebs WN, Engelhardt DW and Cunningham SM 1991 New biostratigraphic age dates from the Lake Rukwa rift basin in western Tanzania. *AAPG Bull*. 75: 1255-1263.

Withjack MO and Jamison WR 1986 Deformation produced by oblique rifting. *Tectonophysics* 126(2-4): 99-124.